

## Single-crystal copper films on sapphire

Janssen, G. C.A.M.; van der Pers, N. M.; Hendriks, R. W.A.; Böttger, A. J.; Kwakernaak, C.; Rieger, B.; Sluiter, M. H.F.

**DOI**

[10.1016/j.tsf.2020.138137](https://doi.org/10.1016/j.tsf.2020.138137)

**Publication date**

2020

**Document Version**

Final published version

**Published in**

Thin Solid Films

**Citation (APA)**

Janssen, G. C. A. M., van der Pers, N. M., Hendriks, R. W. A., Böttger, A. J., Kwakernaak, C., Rieger, B., & Sluiter, M. H. F. (2020). Single-crystal copper films on sapphire. *Thin Solid Films*, 709, Article 138137. <https://doi.org/10.1016/j.tsf.2020.138137>

**Important note**

To cite this publication, please use the final published version (if applicable).  
Please check the document version above.

**Copyright**

Other than for strictly personal use, it is not permitted to download, forward or distribute the text or part of it, without the consent of the author(s) and/or copyright holder(s), unless the work is under an open content license such as Creative Commons.

**Takedown policy**

Please contact us and provide details if you believe this document breaches copyrights.  
We will remove access to the work immediately and investigate your claim.



## Single-crystal copper films on sapphire

G.C.A.M. Janssen<sup>a,\*</sup>, N.M. van der Pers<sup>b</sup>, R.W.A. Hendriks<sup>b</sup>, A.J. Böttger<sup>b</sup>, C. Kwakernaak<sup>b</sup>, B. Rieger<sup>c</sup>, M.H.F. Sluiter<sup>b</sup>

<sup>a</sup> Precision and Microsystems Engineering, 3ME, TU Delft, Mekelweg 2, 2628 CD Delft, the Netherlands

<sup>b</sup> Materials Science & Engineering, 3ME, TU Delft, Mekelweg 2, 2628 CD Delft, the Netherlands

<sup>c</sup> Imaging Physics, Applied Sciences, TU Delft, Lorentzweg 1, 2628 CJ Delft, the Netherlands

### ARTICLE INFO

#### Keywords:

Sapphire  
Aluminum trioxide  
Corundum  
Copper  
Thin film  
Single-crystal  
Oxygen  
Dissolution

### ABSTRACT

Single-crystal copper films on sapphire have recently been reported upon in relation to graphene growth on these films. In the present paper the kinetics of the formation of single crystal copper films is investigated. We demonstrate the importance of heating the sapphire substrate in 1000 hPa oxygen, followed by a fast cooling prior to depositing the copper film. The importance of this treatment is tentatively explained by the dissolution of oxygen in sapphire and subsequent out-diffusion during recrystallization of the copper film to form a copper-oxide interface layer. Also, the importance of avoiding oxygen incorporation in the sputter deposited film is demonstrated.

### 1. Introduction

Sputter deposited copper thin films on amorphous substrates usually consist of equiaxed grains with grain width equal to the film thickness. The 111 crystal planes of the copper film are parallel to the surface [1]. On amorphous substrates no in-plane orientation of the grains exists. In X-ray diffraction (XRD) this shows up as a ring in the 111-pole figure plus a peak in the center. Sputter deposited copper films on single-crystal sapphire however, exhibits local epitaxy, as evidenced by 6 maxima in the 111-pole figure instead of a ring. The 6 maxima stem from two domains in the copper each giving rise to 3 maxima. Between the two domains a twin relation exists. Recently it has been reported that a copper films on sapphire can be transformed into a single-crystal films, as evidenced by 3 maxima in the 111-pole figure [2-5].

Copper on sapphire has a rich history in surface-science. The formation of the first few layers has been investigated thoroughly. See, e.g. Fu et al. [6] and references therein.

In literature two orientation relations between sapphire and copper are mentioned [7]. These relations are between families of directions:  $\langle 1\bar{1}0 \rangle_{Cu}$  and  $\langle 10\bar{1}0 \rangle_{Al_2O_3}$ . Here we choose to present the orientation relations between directions in the sapphire and the copper to emphasize the options for twins.

$$OR-I \equiv (111)_{Cu} \parallel (0001)_{Al_2O_3} \wedge [\bar{1}10]_{Cu} \parallel [\bar{1}010]_{Al_2O_3}$$

$$OR-II \equiv (111)_{Cu} \parallel (0001)_{Al_2O_3} \wedge [\bar{1}10]_{Cu} \parallel [2\bar{1}\bar{1}0]_{Al_2O_3}$$

(0001) sapphire has a six-fold symmetry, while (111) copper has a threefold symmetry. This results for each of the two orientation relations in a physical equivalent orientation relation which has a twin relation to the above-mentioned orientation relations:

$$OR-I' \equiv (111)_{Cu} \parallel (0001)_{Al_2O_3} \wedge [\bar{1}01]_{Cu} \parallel [\bar{1}010]_{Al_2O_3}$$

$$OR-II' \equiv (111)_{Cu} \parallel (0001)_{Al_2O_3} \wedge [\bar{1}01]_{Cu} \parallel [2\bar{1}\bar{1}0]_{Al_2O_3}$$

In all our experiments we observe OR-I and OR-I' with sometimes a minute fraction OR-II and OR-II'. The two OR-types differ slightly in the misfit between the copper and sapphire, albeit that in OR-I the distance between the Cu-atoms is about equal to the distance between Al-atoms, while in OR-II the distance between the Al-atoms is about twice the distance between the Cu-atoms. The distance between two Cu-atoms along  $\langle \bar{1}10 \rangle$  is 0.2556 nm. The distance between two Al-atoms along  $\langle \bar{1}010 \rangle$  is 0.2748 nm. The misfit in OR-I is 7%, with the distance between the Cu-atoms being smaller than the distance between the Al-atoms. In OR-II we need to compare twice the distance between two Cu-atoms along  $\langle \bar{1}10 \rangle$ , i.e. 0.5112 nm with the distance between two Al-atoms along  $\langle 2\bar{1}\bar{1}0 \rangle$ , i.e. 0.4759 nm. In this case the distance between the Cu-atoms is 7% larger than the distance between the Al-atoms.

The present paper deals with the formation of 0.7  $\mu\text{m}$  thick single-crystal copper films on sapphire. Miller et al. [2], Verguts et al. [3], Deng et al. [4] and Huet and Raskin [5] have reported on these films earlier. In refs [2,4,5] the importance of an oxygen pre-treatment of the sapphire is shown. Verguts et al. [3] achieve single crystal films by

\* Corresponding author.

E-mail address: [G.C.A.M.Janssen@tudelft.nl](mailto:G.C.A.M.Janssen@tudelft.nl) (G.C.A.M. Janssen).

hydroxylation of the substrate. Miller et al. [2] have shown the importance of temperature control during sputter deposition of the copper film.

We looked at the pre-treatment of the substrate in detail. We discuss that it is not only the high temperature but also the oxygen pressure and the cooling rate that are important for the achievement of single-crystal films. We explain the importance of temperature control during sputter deposition from the incorporation of oxygen in the film. Finally, we report on the kinetics of the formation of a single crystal copper film.

The copper films, discussed in the present paper, are deposited by sputter-deposition on a sapphire substrate that has undergone a heat pre-treatment in oxygen. The deposited copper films demonstrate local epitaxy, showing both OR-I and OR-I' (6 maxima in the 111 pole-figure, plus one in the center). Heating the sample in an argon-hydrogen atmosphere results in growth of one of the two domains at the expense of the other, resulting in a single crystal copper film (3 maxima in the 111 pole-figure, plus one in the center).

## 2. Experimental

### 2.1. Substrate pre-treatment

Single crystal  $\alpha$ -Al<sub>2</sub>O<sub>3</sub> (0001) plates (10 mm x 10 mm x 0.5 mm, polished on one side, with a deliberate miscut of 0.5°) were used as substrates. (AdValue Technology, USA). The substrates received a number of distinct heat pre-treatments before deposition of the copper film.

- A: Heating 24 h at 1027 °C in 1.4 10<sup>-2</sup> Pa oxygen, with fast cooling.
- B: Heating 24 h at 1027 °C in 800 hPa oxygen, with fast cooling.
- C: Heating 24 h at 1027 °C in 800 hPa oxygen, with slow cooling.
- D: Heating 2 h at 1027 °C in 1000 hPa oxygen, with fast cooling.
- E: Heating 24 h at 1027 °C in 1.4 10<sup>-2</sup> Pa oxygen, with fast cooling, followed by a moderate heating (120 °C) under vacuum in the sputter deposition system and subsequent exposure to water vapor in the load lock of the sputter deposition system.

The heat treatment prior to deposition of the copper is done in the same custom-built system as used for the recrystallization. The system consists of a quartz vacuum tube closed on one side and pumped on the other side. The base pressure of the system is 2 10<sup>-5</sup> Pa. A tube furnace can slide over the quartz tube allowing for fast heating and cooling. Low pressure annealing was performed by admitting oxygen through a needle valve while pumping on the system by a turbo pump. Annealing at 800 hPa was performed by backfilling the system with oxygen to a pressure of 600 hPa and then sliding the furnace over the quartz tube, leading to an increase in pressure by thermal expansion of the gas. Annealing at 1000 Pa was performed by introducing 500 sccm oxygen through a mass flow controller and keeping the pressure in the system 20 hPa above atmospheric pressure by a needle valve between the system and the exhaust.

### 2.2. Sputter deposition

Samples were transported through air from the pre-treatment set-up to the sputter deposition system. Copper films of 0.7 μm thickness were deposited in a direct current sputter deposition system (AJA, USA) in an argon atmosphere at a pressure of 0.95 Pa. The treated sapphire substrates are placed on a heated rotating substrate table. The deposition rate is 0.2 nm/s. The background pressure in the system is 2 10<sup>-5</sup> Pa. The substrate table is heated by two lamps placed below the table. The power to the lamps is controlled by a thermocouple placed in between the lamps and the table. Since the thermal time constant of the thermocouple is much shorter than the thermal time constant of the substrate table the temperature of the table varies over the duration of the deposition. A deposition run is started by setting the temperature to

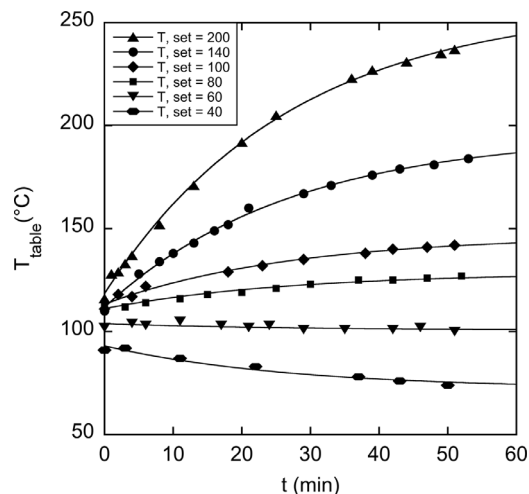


Fig. 1.. Temperature of the substrate table during deposition of copper films for various set temperatures. The lines are fits to the datapoints of the function:  $T = m_1 + m_2(1 - \exp(-m_3t))$ , following from a simple heat flow model.

200 °C. In about five minutes the temperature reading on the thermocouple will overshoot over 200 °C. At that time the set temperature is reduced to the desired temperature. Once the temperature on the control thermocouple has reached that temperature the deposition is started. In Fig. 1 we show temperature measurements of the substrate table by a thermocouple clamped to the substrate table done in a separate experiment at the same argon pressure as used during deposition but without table rotation and without plasma. In the results section we will refer to the set temperatures. In Table 1 we show the average substrate table temperature during the deposition time as function of the set temperature.

### 2.3. Recrystallization

By heating the samples in an argon hydrogen atmosphere one of the two domains increases at the expense of the other. Recrystallization experiments were done in an argon hydrogen mixture at 1000 hPa. Flows of 300 sccm of argon and hydrogen were admitted by mass flow controller. Pressure was kept 20 hPa above atmospheric pressure by a needle valve between the system and the exhaust. Recrystallization experiments were done for 0.5 h, 1 h, and 2 h. at T = 1027 °C. We also did 1 h recrystallization experiments at various temperatures.

### 2.4. Characterization techniques

In order to characterize the films, we used optical microscopy for the appearance of the film: Leica DML. We made use of optical interference microscopy, a technique that is sensitive to height differences and allows to overview large areas before taking an image. For larger magnifications we applied Scanning Electron Microscopy (SEM): Jeol

Table 1.

The average temperature of the substrate table during the time of a deposition for the used set-temperatures.

T <sub>set</sub> (°C)	T <sub>average</sub> (°C)
40	82
60	102
80	121
100	131
120	147
140	157
200	195

JSM-6010LA at 5kV. A third microscopic technique that we used was Atomic Force Microscopy (AFM): Oxford Instruments Cypher S in tapping mode. This technique has a very high sensitivity for height differences, but does not allow to overview large areas before taking an image.

For the crystal structure of the film we used X-ray diffraction, most notably to determine the fractions of the various crystallites in the film and the orientation relation with the sapphire substrate: Bruker D8 Discover with Eulerian cradle, goniometer radius 300mm, X-ray tube Co K $\alpha$ , wavelength 0.17903 nm, 45kV, 25 mA, beam size  $1 \times 1 \text{ mm}^2$ , divergence  $0.25^\circ$ . Diffracted beam side: Parallel sollerslit, divergence  $0.35^\circ$ , graphite monochromator, scintillation detector. The pole figures were obtained by fixing  $\theta - 2\theta$  to the Cu 111 refraction. The rotational angle, phi is scanned from 0 to  $360^\circ$  in steps of  $1^\circ$ . The tilt angle psi is scanned from  $65\text{--}75^\circ$  in steps of  $1^\circ$ . Electron Backscatter Diffraction (EBSD) was used to map out the various crystal orientations in the as deposited film: Jeol JSM 6500F hot field emission gun, Oxford-HKL Nordlys II detector with Channel 5 post processing software.

### 3. Results

#### 3.1. Sputter deposition

In Fig. 2a–c we present optical micrographs (Leica DML) of copper thin films deposited at  $T_{\text{set}}$  is  $40^\circ\text{C}$ ,  $80^\circ\text{C}$  and  $140^\circ\text{C}$  on sapphire pretreated in low pressure oxygen (treatment A), after recrystallization annealing at  $1027^\circ\text{C}$  for 1 h in 1000 hPa argon-hydrogen. In the film deposited at  $40^\circ\text{C}$  deep grooves extending all the way to the substrate have formed. In films deposited at  $T_{\text{set}}$  is  $60^\circ\text{C}$ ,  $80^\circ\text{C}$  and  $100^\circ\text{C}$  the grooves are much less pronounced, but also small, mostly triangular features are observed, black under the interference microscope. These features are identified as non-recrystallized parts of the film. In Fig. 3 we present a SEM micrograph of one of these triangular areas in the film deposited at  $80^\circ\text{C}$  (Jeol JSM-6010LA). The film deposited at  $T_{\text{set}} = 140^\circ\text{C}$  does not show any non-recrystallized parts. The only defects visible under the optical microscope are shallow grain boundaries. The shape of the grooves is a testimony to the hexagonal structure of the sapphire (0001) substrate.

Films deposited at  $200^\circ\text{C}$  show slightly deeper grooves after recrystallization than the films deposited at  $140^\circ\text{C}$ .

In order to quantify the non-recrystallized fraction of the copper film we wrote a computer code to measure the area of the black features for 15 optical micrographs per sample. In Fig. 4 we present the fractional non-recrystallized area as function of the average temperature during deposition of the copper film. It is observed that for higher temperatures a lower fraction of non-recrystallized film is obtained.

In Fig. 5 we present EBSD measurements on a film deposited at  $140^\circ\text{C}$  on a substrate pretreated in high-pressure oxygen (treatment D) without any further treatment (SEM: Jeol JSM 6500F hot Field Emission Gun, EBSD: Oxford-HKL Nordlys II detector with Channel 5 post

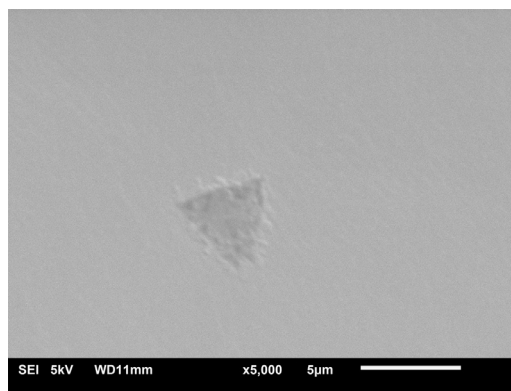


Fig. 3... SEM micrograph of non-recrystallized area in the sample deposited at  $T_{\text{set}} = 80^\circ\text{C}$ .

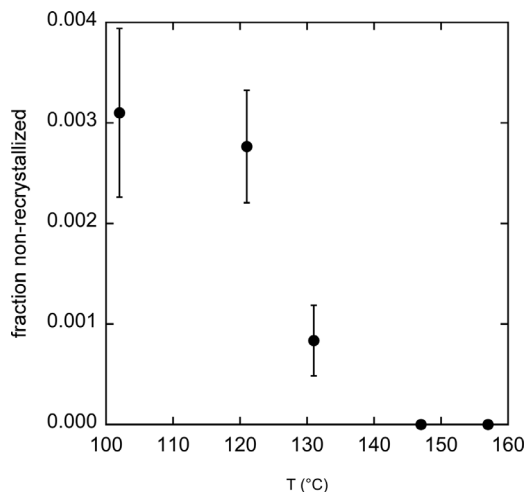


Fig. 4. Fractional area of non-recrystallized film as function of the average temperature during deposition.

processing software). The red and blue areas represent the two domains of the copper film. Both domains have the 111 planes parallel to the surface and exhibit local epitaxy to the sapphire (OR-I and OR-I'). For the sample presented in Fig. 5 we present the XRD 111 pole figure in Fig. 6a (Bruker D8 Discover with parallel beam geometry, height 1mm, width 1 mm, Co K $\alpha$ , 45 kV, 25 mA). The six maxima in Fig. 6(a) indicate two domains in the film with local epitaxy to the sapphire. From the data underlying the XRD 111 pole figure, presented in Fig. 6a it is seen that on this sample the two fractions are not equal, the distribution OR I/ORI' is 55/45.

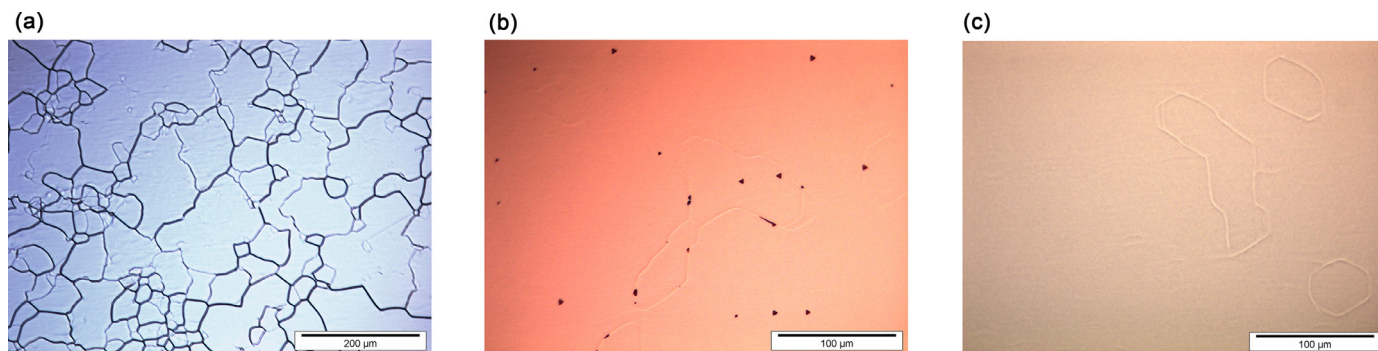


Fig. 2.. Optical micrographs of  $0.7 \mu\text{m}$  thick copper films deposited on sapphire at  $T_{\text{set}} = 40^\circ\text{C}$  (a),  $80^\circ\text{C}$  (b) and  $140^\circ\text{C}$  (c), after subsequent annealing for 1h at  $1027^\circ\text{C}$  in a flowing argon hydrogen mixture of 300 sccm Ar/ 300 sccmH $_2$  at 1000 hPa.

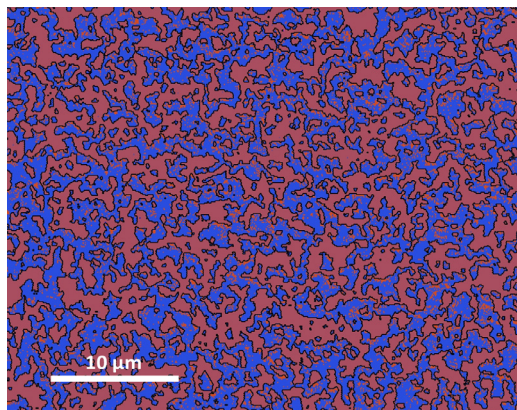


Fig. 5.. EBSD measurement of a film deposited at  $T_{\text{set}} = 140$  °C. The red and blue areas are the two orientations (OR-I and OR-I') in the copper film, between which a twin relation exists.

### 3.2. Recrystallization

We have studied the dependence of recrystallization on the pre-treatment of the sapphire for films deposited at  $T_{\text{set}} = 140$  °C. For films with pre-treatment B and D single-crystal copper was realized by annealing for 1 h in 1000 hPa argon-hydrogen at 1027 °C, as witnessed by the 111 pole-figure in Fig. 6b. The three maxima in Fig. 6(b) indicate a single-crystal film. For the films deposited on substrates with pre-treatment A, C, and E no single crystal copper was achieved.

For Cu films deposited at 140 °C on sapphire with pretreatment D (high pressure, fast cooling) we studied the recrystallization in detail. In Fig. 7 we present the recrystallized fraction as function of the annealing temperature for an annealing time of 1 h. The recrystallized fraction is defined as the sum of the intensities of the three peaks pertaining to the dominant domain divided by sum of all six peaks. The recrystallized fraction runs from  $\frac{1}{2}$  (no preferential orientation) to 1 (single-crystal). For temperatures up to 500 °C the recrystallized fraction increases steadily with annealing temperature. Between 550 °C and 650°C the recrystallized fraction increases rapidly but not perfectly reproducibly. Above 650° the last part of the film recrystallizes to reach almost complete recrystallization at 1027 °C.

In Fig. 8 we present an AFM image of a 0.7 μm thick copper film on sapphire (treatment D), deposited at  $T_{\text{set}} = 140$  °C after annealing at

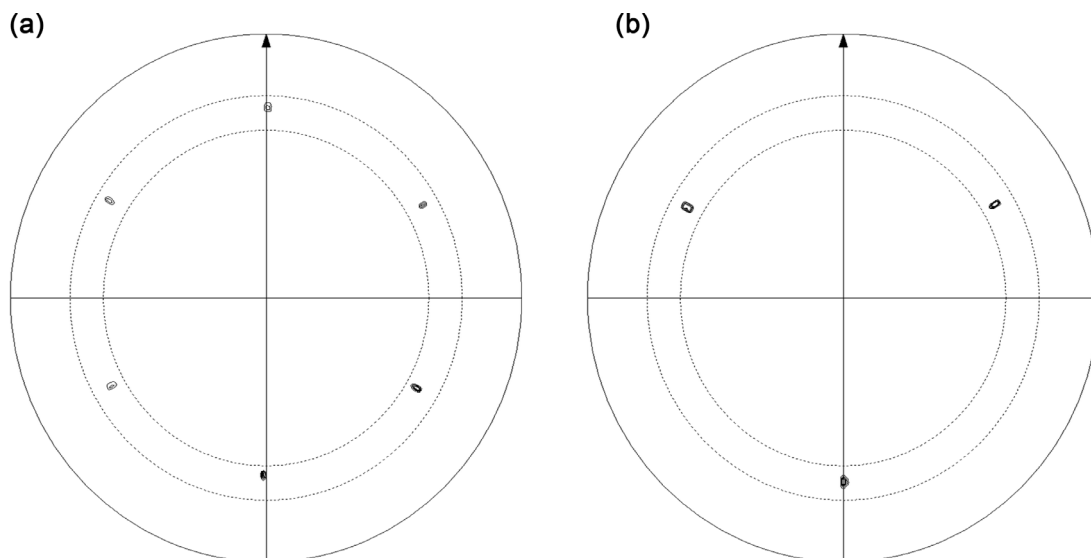


Fig. 6. 111 pole-figure of the as deposited copper film (a) and of a copper film recrystallized at 1027 °C for 1 h (b). The sapphire was pretreated for 2 h in atmospheric pressure oxygen and fast cooled. The copper film was deposited at  $T_{\text{set}} = 140$  °C.

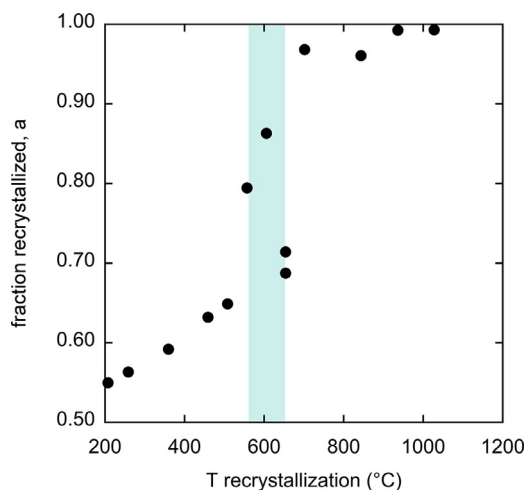


Fig. 7.. Fraction recrystallized,  $a$ , as function of the temperature of annealing for 1h. By annealing at temperatures 200 °C to 500 °C the fraction increases steadily from 55% to 65%. At a temperature between 550 °C and 650 °C a fast increase is observed. From 700 °C to 1027 °C the increase is moderate.

1027 °C for 1 h. The three sets of lines, visible in the picture, making angles of 60° with each other are steps of 0.5 to 1.0 nm high. These steps are due to dislocations, caused by the misfit of the copper on the sapphire.

In Fig. 9 we present optical micrographs of 0.7 μm copper films on sapphire (treatment D), deposited at  $T_{\text{set}} = 140$  °C after annealing at 1027 °C for 30 min(9a), 1 h (9b) and 2 h (9c). The recrystallization after 30 min is 96%, after 1 h it is 99%. The recrystallization deteriorates thereafter. After 2 h the recrystallization is only 59%. The roughness increases continuously with time. In Fig. 9a we needed a defect to show the microscope was in focus. In Fig. 9b we see some indication of grooves forming, In Fig. 9c the grooves are abundant.

## 4. Discussion

### 4.1. Substrate preparation

The achievement of single crystal copper depends critically on substrate preparation. Traditionally, annealing of sapphire in an oxygen

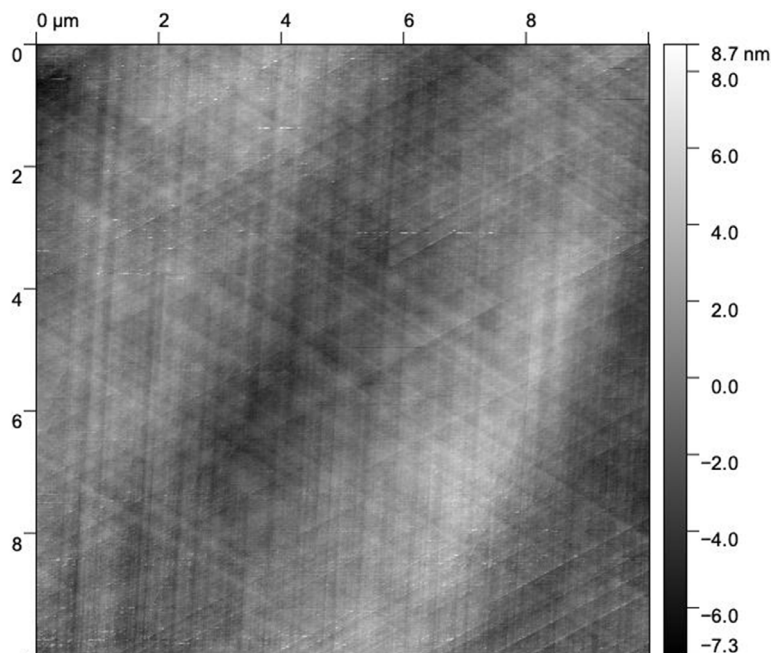


Fig. 8.. AFM image (10  $\mu\text{m}$  x 10  $\mu\text{m}$ ) of a copper film on sapphire after 1 h annealing at 1027  $^{\circ}\text{C}$ . The regular line patterns are steps of 0.5 to 1.0 nm due to dislocations, caused by the misfit between the copper and the sapphire.

atmosphere has been done to make sure that the sapphire is oxygen terminated. Here we claim that it is not only the surface termination, but also the dissolution of some oxygen in the sapphire that is important for the achievement of single crystal copper films, see the section on recrystallization below. In order to get some oxygen dissolved in the sapphire sample it must be heated in “high pressure” oxygen to have enough driving force for dissolution. Secondly in order not to lose the oxygen during cooling of the samples we need “fast” cooling in order to kinetically prevent the out-diffusion of oxygen. We argue that the procedures B and D lead to dissolved oxygen and the procedures A, C, and E, do not. It is only with samples that have received either procedure B or D that we achieved single crystal copper films. Procedure E was intended to prepare the sapphire in a hydroxylated state. Both Verguts et al. [3] for experiments comparable to ours as well as Fu et al. [6] for few atomic layer surface science experiments argue that hydroxylation is important. Verguts et al. reach this by boiling acid, while Fu et al. reach this by exposing the sample in the load-lock to water vapor. We were not successful in reaching single crystal copper by procedure E. In fact, we obtained grains ranging from 50 to 200 micron separated by deep grooves, suggesting that too much water was used, leading to an oxygen contaminated copper film.

#### 4.2. Sputter deposition

We explain the effect of substrate table temperature during sputter deposition on film morphology after recrystallization on the amount of oxygen incorporated in the growing film. The background pressure of  $2 \cdot 10^{-5}$  Pa consists almost completely on water. If the sticking coefficient were one, we would get a monolayer of water every five seconds. This combined with a growth rate of two monolayers of copper per second would give an oxygen contamination of 10%. In reality the sticking may be less, but it is possible to incorporate appreciable amounts of oxygen in the copper film. The amount of water,  $\sigma$ , on a clean surface is proportional to the fraction of water molecules that have insufficient energy to escape from the surface (modified after de Boer [8]):

$$\sigma = C e^{\frac{Q}{kT}} \quad (1)$$

with  $Q$  the desorption energy of a water molecule. The temperature dependent coverage with water of a clean copper surface is described by Eq. (1), with  $Q=0.58$  eV [9]

Deposition at elevated temperature will decrease the amount of oxygen incorporated in the growing film and thereby the amount of non-recrystallized film after annealing (Fig. 4). We do not obtain a dependence as straightforward as Eq. (1) (Fig. 4). As an explanation we

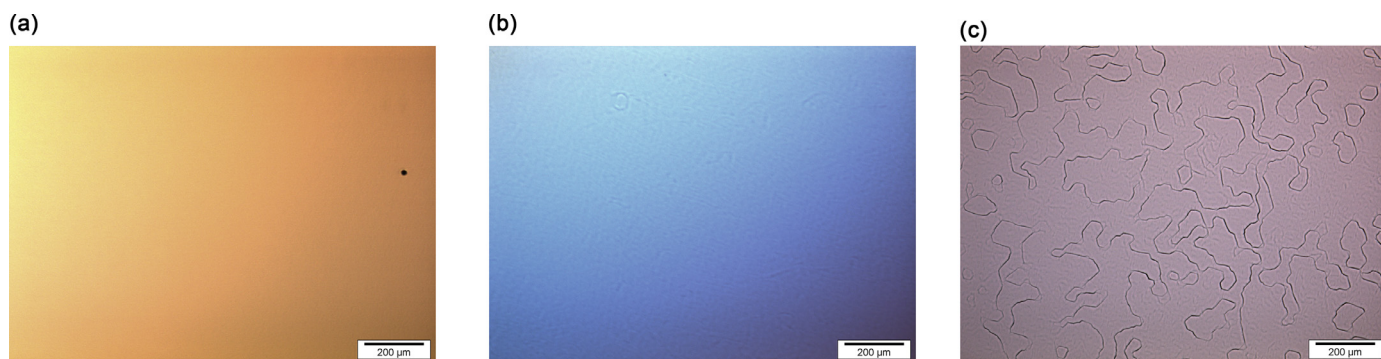


Fig. 9. a, b, c: Copper films on sapphire after annealing at 1027  $^{\circ}\text{C}$  for 30 min, 1 h and 2 h. The fraction recrystallized material first goes up 96%, 99% and then goes down: 59%. The roughness goes up monotonously with time at elevated temperature.

suggest that the adsorption kinetics may saturate at a coverage of one monolayer or even a fraction thereof for low temperatures, and the adsorption kinetics on a growing film may differ from the adsorption kinetics on a clean surface.

Heating of the substrate, however, has the same effect on the growing film as heating the windshield in your car has on the amount of water on the windshield. By heating the windshield you do not diminish the amount of water in your car, but it will no longer sit on the windshield. The same happens for the growing copper film.

We argue that during recrystallization the oxygen in the film is not incorporated in the growing domain, but is pushed forward, until the local concentration of oxygen becomes so high that the recrystallization stops. Therefore, we argue that the amount of oxygen in the film is proportional to the non-recrystallized fraction of the surface. In Fig. 4 we presented the fraction of non-crystallized film as function of the average temperature during deposition. At  $T = 102\text{ }^{\circ}\text{C}$  and  $T = 121\text{ }^{\circ}\text{C}$  the fractional non-recrystallized area is equal. Tentatively this may have to do with a change in adsorption once a certain coverage is reached.

#### 4.3. Recrystallization

In Fig. 7 the recrystallization is presented for annealing for 1 h as function of the annealing temperature. We define the fraction recrystallized ( $a$ ) as the sum of the intensities of the three X-ray texture peaks associated with the dominant domain divided by the sum of the intensities of all six peaks. In order to model the recrystallization and to extract an activation energy for the rate limiting process we need to make an assumption on the rate of  $a$  as function of  $a$ . We make the first order assumption that the rate of recrystallization is proportional to the non-recrystallized fraction. Moreover, we assume that the recrystallization is thermally activated.

$$\frac{da}{dt} = C e^{-\frac{Q}{kT}} (1 - a) \quad (2)$$

Rearranging and integrating:

$$\int_{1/2}^a \frac{1}{1 - a'} da' = C e^{-\frac{Q}{kT}} \int_0^t dt' \quad (3)$$

$$\ln\left(\frac{1}{2}\right) - \ln(1 - a) = C t e^{-\frac{Q}{kT}} \quad (4)$$

Taking another logarithm:

$$\ln\left(\ln\left(\frac{1}{2}\right) - \ln(1 - a)\right) = \ln(C) + \ln(t) + \frac{-Q}{kT} \quad (5)$$

By plotting  $\ln(\ln(\frac{1}{2}) - \ln(1 - a))$  as a function of  $1/T$  we obtain  $Q$  from the slope of the curve. In Fig. 10 the data are presented according to this recipe. A straight line is fitted to the five data points from  $200\text{ }^{\circ}\text{C}$  to  $500\text{ }^{\circ}\text{C}$ . an activation energy of  $0.13\text{ eV}$  is obtained. We argue that the  $0.13\text{ eV}$  we have obtained is the activation energy for grain boundary movement, more precisely the hindering of grain boundary movement in the copper by the sapphire.

We explain the acceleration of recrystallization above  $550\text{ }^{\circ}\text{C}$  from the formation of a CuO interface layer formed by oxidizing the first few monolayers of copper near the sapphire by oxygen out-diffusing from the sapphire. This CuO interface layer was observed by Deng et al. [4]. Combining the observation that only substrate pretreatment in high temperature oxygen, followed by fast cooling leads to single-crystal copper films, with the observation by Deng et al. of a CuO interface layer and the acceleration of the recrystallization above  $550\text{ }^{\circ}\text{C}$ , while knowing that oxygen is avoided during processing except in the substrate pretreatment, leads us tentatively to conclude that some oxygen must be dissolved in the sapphire. This small amount of oxygen is crucial in obtaining single-crystal copper films, since during the formation of the CuO interface layer the grain boundaries in the copper are

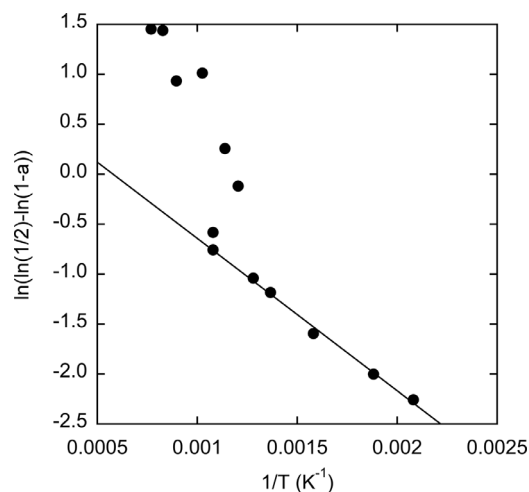


Fig. 10.. Replot of the data presented in Fig. 7. A linear fit has been made to the datapoints at the lowest five temperatures.

no longer pinned. The oxygen of the CuO layer observed by Deng et al. [4] has to come with the substrate. It is difficult to find another way to bring the oxygen along other than by dissolution.

In Fig. 9c it is shown that prolonged annealing of the copper film on sapphire leads to poly-crystallization. We offer no detailed explanation for this effect. We assume that poly-crystallization allows for annihilation of some of the dislocations responsible for the steps shown in Fig. 8, with a favorable energy trade-off.

## 5. Conclusions

Single crystal copper films on sapphire have been reproducibly obtained. Two steps turned out to be critically important: First, a high temperature, high pressure oxygen treatment of the substrates, followed by a fast cooling. This step is tentatively explained to be responsible for dissolving a small amount of oxygen in the sapphire. During recrystallization of the copper film the oxygen diffuses out of the sapphire to form a copper-oxide interface layer. Second, avoiding oxygen contamination of the copper film.

### CRedit authorship contribution statement

**G.C.A.M. Janssen:** Conceptualization, Investigation, Writing - original draft. **N.M. van der Pers:** Formal analysis, Investigation, Data curation. **R.W.A. Hendriks:** Formal analysis, Investigation, Data curation. **A.J. Böttger:** Investigation, Formal analysis. **C. Kwakernaak:** Formal analysis, Investigation, Data curation. **B. Rieger:** Investigation, Software. **M.H.F. Sluiter:** Conceptualization, Investigation.

### Declaration of Competing Interest

The authors declare that they have no known competing financial interests or personal relationships that could have appeared to influence the work reported in this paper.

### Acknowledgements

We gratefully acknowledge the support from the technical staff of PME, most specially Harry Jansen, Patrick van Holst and Gideon Emmaneel for constructing the equipment. Furthermore, we thank Yuwei Chen and Hanqing Liu for operating the AFM.

This research did not receive any specific grant from funding agencies in the public, commercial, or not-for-profit sectors. It was completely paid for by the Technical University Delft.

## References

- [1] L.B. Freund, Subra Suresh, *Thin Film Materials: Stress, Defect Formation and Surface Evolution*, Cambridge University Press, 2004.
- [2] David L. Miller, Mark W. Keller, Justin M. Shaw, Katherine P. Rice, Robert R. Keller, Kyle M. Diederichsen, Giant secondary grain growth in Cu films on sapphire, *AIP Adv.* 3 (2013) 082105, <https://doi.org/10.1063/1.4817829>.
- [3] Ken Verguts, Bart Vermeulen, Nandi Vrancken, Koen Schouteden, Chris Van Haesendonck, Cedric Huyghebaert, Marc Heyns, Stefan De Gendt, Steven Brems, Epitaxial AlO (0001)/Cu (111) template development for CVD graphene growth, *J. Phys. Chem. C* 120 (2016) 297–304, <https://doi.org/10.1021/acs.jpcc.5b09461>.
- [4] B. Deng, Z. Pang, S. Chen, X. Li, C. Meng, J. Li, M. Liu, J. Wu, Y. Qi, W. Dang, H. Yang, Y. Zhang, J. Zhang, N. Kang, H. Xu, Q. Fu, X. Qiu, P. Gao, Y. Wei, Z. Liu, H. Peng, Wrinkle-free single-crystal graphene wafer grown on strain-engineered substrates, *ACS Nano* 11 (2017) 12337–12345, <https://doi.org/10.1021/acsnano.7b06196>.
- [5] Benjamin Huet, Jean-Pierre Raskin, Role of Cu substrate in the growth of ultra-flat crack-free highly-crystalline single-layer graphene, *Nanoscale* 10 (2018) 221898–221909, <https://doi.org/10.1039/c8nr06817h>.
- [6] Q. Fu, T. Wagner, M. Rühle, Hydroxylated  $\alpha$ -AlO (0 0 0 1) surfaces and metal/ $\alpha$ -Al<sub>2</sub>O<sub>3</sub> (0 0 0 1) interfaces, *Surf. Sci.* 600 (2006) 4870–4877, <https://doi.org/10.1016/j.susc.2006.08.008>.
- [7] G. Dehm, H. Edongue, T. Wagner, S.H. Oh, E. Arzt, Obtaining different orientation relationships for Cu films grown on (0001)  $\alpha$ -Al<sub>2</sub>O<sub>3</sub> substrates by magnetron sputtering, *Z. Metallkunde* 96 (2005) 249–254, <https://doi.org/10.3139/146.101027>.
- [8] J.H. de Boer, *The Dynamical Character of Adsorption*, 2nd ed., Oxford University Press, London, 1968, p. 45.
- [9] B.J. Hinch, L. Dubois, Stable and metastable phases of water adsorbed on Cu(111), *J. Chem. Phys.* 96 (1992) 3262, <https://doi.org/10.1063/1.461971>.